3.2

Distinct perfusion patterns in Alzheimer's disease, frontotemporal dementia and dementia with Lewy Bodies

Maja A.A. Binnewijzend, Joost P.A. Kuijer, Wiesje M. van der Flier,
Marije R. Benedictus, Christiane Möller, Yolande A.L. Pijnenburg, Afina W. Lemstra,
Niels D. Prins, Mike P. Wattjes, Bart N.M. van Berckel,
Philip Scheltens, Frederik Barkhof

Submitted

ABSTRACT

Objective: To compare pseudo-continuous arterial spin-labeled (PCASL) magnetic resonance imaging (MRI) measured quantitative cerebral blood flow (CBF) of patients with frontotemporal dementia (FTD), dementia with Lewy Bodies (DLB), Alzheimer's disease (AD) and controls, in a region-of-interest (ROI) and voxel-wise fashion.

Design: We analyzed whole-brain 3D fast-spin-echo PCASL images of 20 FTD patients, 14 DLB patients, 48 AD patients and 50 subjects with subjective complaints who served as controls from the memory clinic based Amsterdam Dementia Cohort. Regional CBF patterns were compared using analyses-of-variance for repeated measures. Permutation tests were used for voxel-wise comparisons. Analyses were performed using uncorrected and partial volume corrected (PVC) maps. All analyses were corrected for age and sex.

Results: There was an interaction between diagnosis and region ($p<0.001$), implying differences in regional CBF changes between diagnostic groups. In AD patients, CBF was decreased in all supratentorial regions, most prominently so in the posterior regions, and least prominently in the frontal lobes. DLB patients showed lowest CBF values throughout the brain, but temporal CBF was preserved. FTD patients showed moderate CBF decreases in all brain regions, except for the temporal lobes. Supratentorial PVC cortical CBF values were lowest in the frontal lobes in FTD patients, and in the temporal lobes in AD patients.

Conclusion: Distinct patterns of quantitative regional CBF changes occur in patients with AD, FTD and DLB. 3D-PCASL may provide additional value in the workup of dementia patients and the differentiation between the most common types of neurodegenerative disorders that underlie dementia.

INTRODUCTION

Alzheimer's disease (AD) is the most common cause of dementia, accounting for 50-60% of dementia cases, followed by dementia with Lewy Bodies (DLB) and frontotemporal dementia (FTD) that account for approximately 15-25% of cases.[1] Although clinical symptoms differ among all three conditions, in clinical practice there is a large amount of overlap, especially in the earliest phase.[2-4] Similarly, cortical atrophy patterns on structural MRI vary among the three conditions. In line with their pathological substrates, atrophy is mainly seen in the medial temporal and parietal cortices in AD patients,[5] and in the frontotemporal cortices in FTD patients.[6] DLB patients tend to display a more diffuse pattern of cortical atrophy, with a relative preservation of the medial temporal lobe area compared to AD patients.[7] However, again, overlap may be present, and atypical patterns are seen in all conditions. Furthermore, atrophy may be completely absent in the earliest phase.[8] These factors hamper the contribution of structural MRI to the differential diagnosis in an early stage of the disease.

Functional changes generally preceed actual gray matter volume loss, and can be detected by using functional neuroimaging.[8] Single-photon emission computed tomography (SPECT) and fluorodeoxyglucose positron emission tomography (FDG-PET) allow assessment of cerebral blood flow (CBF) and glucose metabolism respectively and have emerged as potential means to help differentiate between underlying subtypes of dementia.[9-11] Disadvantages of these techniques are the relative insensitivity in the early phase, patient burden because of intravenous injection of radioactive tracers, and costs.

Arterial spin-labeled (ASL) MRI is an alternative functional brain imaging technique that measures cerebral blood flow (CBF) by using magnetically labeled arterial blood water, flowing through the carotid and vertebral arteries, as an endogenous contrast medium. The pseudo-continuous variant of ASL (PCASL) uses a multitude of millisecond-long pulses in order to achieve a high labeling efficiency and effective compensation of magnetization transfer effects.[12] Important advantages of ASL are its non-invasiveness and short acquisition time at higher magnetic field strengths. This allows routine clinical application in the workup of dementia when ASL is added to the standard dementia scanning protocol, which minimizes both patient burden and costs. We previously showed that PCASL discriminates both MCI and AD from controls,[13] illustrating its potential for early diagnosis.

In this study we used quantitative whole-brain PCASL[12] to compare regional CBF distribution patterns in different types of dementia, to investigate its potential use in differential diagnosis.

METHODS

Subjects

In this case-control study, we included 22 patients with behavioral variant FTD (bvFTD), 14 patients with DLB, 48 age-matched patients with AD, and 50 age-matched subjects with subjective complaints that served as controls from the memory clinic based Amsterdam Dementia Cohort. All subjects visited our memory clinic between 10 October 2010 and 10 October 2012. AD patients and controls were selected from a previously published dataset containing 71 AD patients and 73 controls.[13] All patients underwent a standard dementia screening that included medical history, physical and neurological examinations, screening laboratory tests, neuropsychological testing and brain MRI. Clinical diagnosis was established by consensus in a multidisciplinary team. AD patients met the NINCDS-ADRDA criteria for probable AD[2] and were included if cerebrospinal fluid (CSF) amyloid beta (Abeta) was available and consistent with the AD pathophysiological process (< 550 ng/L). Therefore, AD patients met the criteria for probable AD proposed by the National Institute on Aging and the Alzheimer's Association (NIA-AA) workgroup with at least intermediate likelihood.[14] DLB patients fulfilled clinical criteria for probable DLB.[3] Diagnosis of FTD was based on the Neary criteria.[4] Retrospectively, all patients fulfilled the criteria for probable bvFTD according to Rascovsky et al.[15] FTD patients with severe to end-stage asymmetric cortical atrophy of the right anterior temporal pole were not included (n=3). Patients were considered to have subjective complaints when clinical investigations were normal. In addition, they were required to have normal amyloid levels (> 550 ng/L) if CSF was available. There was no CSF data available of 7 controls. The Ethical Review Board of the VU University Medical Center approved the study. All patients provided written informed consent.

MRI acquisition

MRI was performed on a 3T whole body MR system (Signa HDxt, GE Medical Systems Milwaukee, WI, USA) using an 8-channel head coil. Structural images included a sagittal 3D T1-weighted sequence (IR-FSPGR, echo time=3.0ms, repetition time=7.8ms, inversion time=450ms, flip angle=12°, voxel size 1x0.9x0.9mm) for anatomical information, and a sagittal 3D fluid attenuated inversion recovery (FLAIR) sequence (CUBE, echo time=123.6ms, repetition time=8000ms, inversion time=2351ms, echo-train length=230, voxel size 1.2x1x1mm) to determine the severity of vascular white matter hyperintensities (WMH) using the Fazekas scale.[16] PCASL perfusion images (3D-FSE acquisition with background suppression, post-label delay 2.0s, echo time=9ms, repetition time=4.8s, spiral readout 8 arms x 512 samples; 36x5.0mm axial slices,

3.2x3.2mm in-plane resolution, reconstructed pixel size 1.7x1.7mm, acquisition time 4 minutes) were calculated using a single compartment model[17] after the subtraction of labeled from control images. Binnewijzend et al. provides a more detailed description of the ASL sequence.[13]

Pre-processing and MRI data analysis

Both T1-weighted and PCASL images were corrected for gradient non-linearities in all three directions. Further data analyses were carried out using FSL (version 4.1.9; http://www.fmrib.ox.ac.uk/fsl). Pre-processing of T1-weighted images consisted of non-brain tissue removal,[18] linear registration to standard space[19] and tissue segmentation[20] yielding partial volume estimates. Gray matter volumes, normalized for subject head size (NGMV), were estimated.[18] PCASL images were linearly registered to the brain-extracted T1-weighted images. The brain mask was used to calculate uncorrected mean whole brain CBF. Partial volume estimates were transformed to the ASL data space and used in a regression algorithm,[21] using a Gaussian kernel of 9.5mm full width at half maximum, to create PVC cortical CBF maps. Partial volume estimates were subsequently used as a weighting factor to calculate mean cortical CBF. Additionally, the MNI152 atlas and the Harvard-Oxford cortical atlas (both part of FSL) were used to create regions-of-interest (ROIs) of the frontal, temporal, parietal, occipital and cerebellar brain areas, and of the precuneus and posterior cingulate cortex (PPC), to extract mean regional uncorrected and PVC cortical CBF values. One bvFTD patient had to be excluded due to failure of structural image pre-processing. Another bvFTD patient was excluded because CBF calculation failed due to unknown reason. This resulted in a dataset of 20 bvFTD patients, 48 AD patients, 14 DLB patients and 50 controls.

Complementary, voxel-wise comparisons of both uncorrected CBF maps and PVC cortical CBF maps were performed using nonparametric permutation tests (5000 permutations) to detect voxel-wise CBF differences between groups. Analyses were corrected for age and sex. After threshold-free cluster enhancement (TFCE), significant voxels were found by applying a family-wise error (FWE) corrected threshold corresponding to $p = 0.05$.[22, 23]

Statistics

All other statistical analyses were performed using SPSS (version 20; SPSS, Chicago, Ill, USA). For continuous measures, differences between groups were assessed using one-way analyses-of-variance (ANOVA) with post-hoc Bonferroni tests to correct for multiple comparisons. A chi-squared test was used to compare frequency distributions

of sex. Differences in CBF between diagnostic groups were analyzed using ANOVA with post-hoc Bonferroni tests, correcting for the effect of age and sex (model 1), and additionally for WMH (Fazekas-score; model 2). Additionally, regional differences in CBF between subjects with subjective complaints, AD patients, bvFTD patients and DLB patients were assessed using ANOVA for repeated measures entering diagnosis as between-subjects factor and region (frontal, temporal, parietal, PPC, occipital and cerebellum) as within-subjects variables. Age and sex (model 1) and additionally WMH (Fazekas-score; model 2), were entered as covariates.

RESULTS

Demographics and MRI findings are presented in Table 1. DLB patients were less often females than AD patients (p=0.008). There were no differences in age between study groups. Patients with AD and DLB had lower MMSE-scores compared to controls and bvFTD patients (p<0.01). AD patients had more WMH than bvFTD patients and controls (p<0.05). Normalized gray matter volume (NGMV) was lower in all patient groups compared to controls and did not differ between patient groups.

Table 1. Demographics and MR imaging findings.

	Control	AD	bvFTD	DLB
Number	50	48	20	14
Age (yrs)[#]	62±6	65±7	63±7	66±8
Sex (n female)	18 (36%)	26 (54%)	6 (30%)	2 (14%)[b]
MMSE[#]	28±1.7	21±4.6[a,c]	26±2.6	21±3.7[a,c]
WMH[#]	0.6±0.6	1.2±0.9[a,c]	0.6±0.8	1.0±0.8
NGMV (mL)[#]	772±35	713±42[a]	734±35[a]	707±34[a]

[#] Data demonstrated in means and standard deviations. MMSE: mini mental state examination, WMH: white matter hyperintensities (based on Fazekas-score), NGMV: normalized gray matter volume. [a] p<0.05 compared to controls, [b] p<0.05 compared to AD patients, [c] p<0.05 compared to bvFTD patients, [c] p<0.05 compared to bvFTD patients.

Total CBF differences

Total uncorrected CBF and total PVC cortical CBF differed between groups. Post-hoc tests showed that AD patients, DLB patients and bvFTD patients had lower uncorrected

CBF and PVC cortical CBF compared to controls (all p<0.001; Table 2). Moreover, DLB patients showed a trend of lowered PVC cortical CBF (p=0.06) compared to patients with AD. Additional correction for WMH did not essentially change the group differences.

Differences in regional CBF patterns

ANOVA for repeated measures adjusted for age and sex was used to assess the regional CBF distribution patterns of uncorrected CBF and PVC cortical CBF in relation to diagnosis. For both uncorrected CBF and PVC cortical CBF, there was a main effect of diagnosis (p<0.001) and region (trend; p=0.06 and p=0.18 respectively). Moreover, there was an interaction between diagnosis and region (p<0.001), implying that the

Table 2. Region-of-interest based CBF values.

	Control	AD	bvFTD	DLB
Uncorrected CBF (ml/100g/min)				
Total	32±5	27±5^{aaa}	26±7^{aaa}	23±6^{aaa}
Frontal	22±4	19±5^{a}	17±5^{aa}	14±4^{aaa,x}
Temporal	26±5	21±5^{aaa,ccc,d}	27±9	24±6
Parietal	30±5	23±6^{aaa}	24±7^{aa}	18±5^{aaa,c}
PPC	38±6	30±7^{aaa}	30±9^{aaa}	24±6^{aaa}
Occipital	34±7	26±7^{aaa}	27±8^{aa}	21±8^{aaa}
Cerebellum	25±5	24±5	20±7^{a}	19±9^{a}
Partial volume corrected cortical CBF (ml/100g/min)				
Total	49±7	42±8^{aaa}	39±11^{aaa}	33±10$^{aaa,+}$
Frontal	49±8	42±9^{aa}	39±12^{aa}	33±10^{aaa,v}
Temporal	44±6	38±7^{aa,cc}	46±15	41±11
Parietal	56±9	45±10^{aaa}	45±14^{aa}	35±10^{aaa,b,z}
PPC	64±10	53±12^{aaa}	50±16^{aaa}	41±11^{aaa,b}
Occipital	55±9	46±10^{aaa}	43±12^{aaa}	35±11^{aaa,b}
Cerebellum	42±9	39±9	32±11^{aa,v}	30±10^{aa}

Results demonstrated in means and standard deviations. If analysis of variance was p<0.05 a post hoc Bonferroni test was performed. Shown results are corrected for age and sex. CBF: cerebral blood flow, PPC: precuneus and posterior cingulate. ^{a} p<0.05 compared to subjects with subjective complaints, ^{aa} p<0.01 compared to subjects with subjective complaints, ^{aaa} p<0.001 compared to subjects with subjective complaints, ^{b} p<0.05 compared to AD patients, ^{bbb} p≤0.001 compared to AD patients, ^{c} p<0.05 compared to patients with bvFTD, ^{x} p=0.05 compared to patients with AD, $^{+}$ p=0.06 compared to patients with AD, ^{v} p=0.08 compared to patients with AD, ^{z} p=0.07 compared to patients with bvFTD.

regional distribution of CBF changes differed between the diagnostic groups (Figure 1). In AD patients, uncorrected CBF was decreased in all supratentorial brain regions, but most prominently in the posterior part of the brain, i.e., the parietal (mostly PPC) and the occipital lobes, and least outspokenly in the frontal lobes. Compared to the other patient groups, DLB patients showed lowest CBF values in all brain regions, except for the temporal lobes, where CBF was preserved. CBF decreases were most prominent in the posterior brain regions in DLB as well. BvFTD patients also showed CBF decreases in all brain regions, except for the temporal lobes, but CBF decreases were less prominent than in DLB patients. Furthermore, CBF decreases in bvFTD were as outspoken in the frontal brain regions as they were in the posterior brain regions. Finally, supratentorial PVC cortical CBF values were lowest in the frontal lobes in bvFTD patients, and in the temporal lobes in AD patients. Post-hoc comparisons of regional CBF values are displayed in Table 2. Results remained essentially unchanged when adding WMH as an additional covariate.

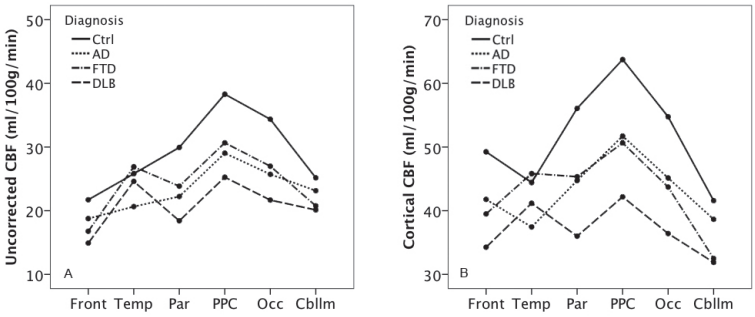

Figure 1. Distinct patterns of cerebral blood flow (CBF) changes according to ANOVA for repeated measures: a) uncorrected CBF, and b) partial volume corrected (PVC) gray matter CBF. Front: frontal lobes, Temp: temporal lobes, Par: parietal lobes, PPC: precuneus and posterior cingulate cortex, Occ: occipital lobes, Cbllm: cerebellum.

Voxel-wise CBF differences

Voxel-wise comparisons confirmed that, compared to controls, most widespread changes were seen in DLB patients, with a pattern of lower uncorrected CBF throughout the brain (Figure 2). In AD patients, uncorrected CBF was also lower compared to controls throughout the brain, but most prominent changes were seen in the posterior cingulate, precuneus and bilateral parietal cortical regions. In bvFTD patients, lower uncorrected CBF compared to controls was more pronounced in the frontal than

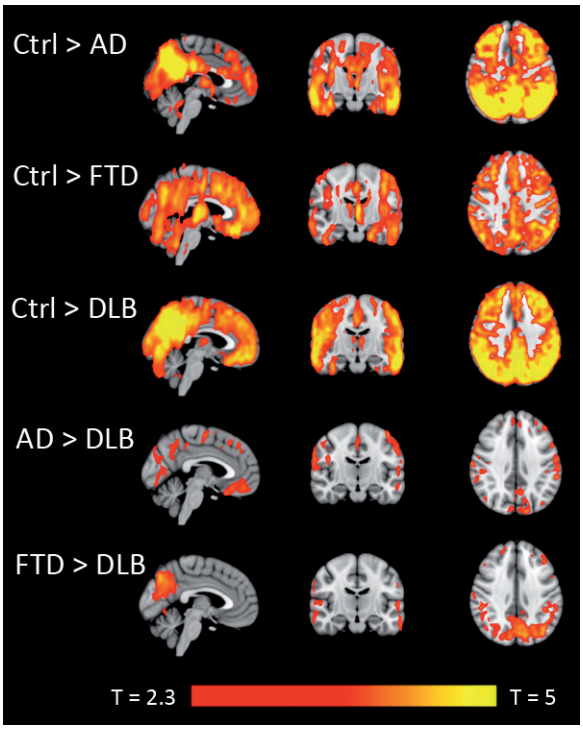

Figure 2. Differences in uncorrected cerebral blood flow (CBF) according to voxel-wise analyses: a) CBF lower in AD compared to controls, b) CBF lower in bvFTD compared to controls, c) CBF lower in DLB compared to controls, d) CBF lower in DLB compared to AD, e) CBF lower in DLB compared to bvFTD. Voxel-wise analysis showed no differences in CBF between DLB and AD patients. Data are presented as T-maps (T>2.3, corresponding to FWE-corrected p<0.05). MNI coordinates (x=-3,y=-15,z=36).

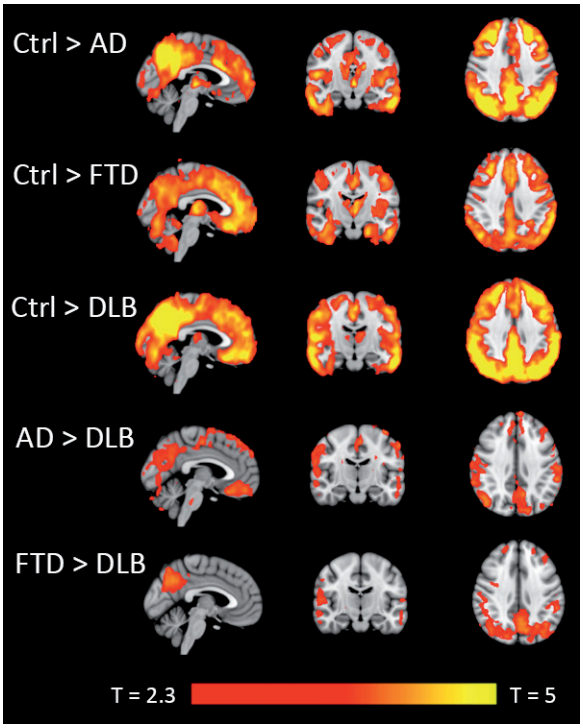

Figure 3. Differences in partial volume corrected (PVC) cortical cerebral blood flow (CBF) according to voxel-wise analyses: a) CBF lower in AD compared to controls, b) CBF lower in bvFTD compared to controls, c) CBF lower in DLB compared to controls, d) CBF lower in DLB compared to AD, e) CBF lower in DLB compared to bvFTD. Voxel-wise analysis showed no differences in CBF between DLB and AD patients. Data are presented as T-maps (T>2.3, corresponding to FWE-corrected p<0.05). MNI coordinates (x=-3,y=-15,z=36).

the posterior regions. No regions of higher CBF were detected in the patient groups compared to the control group. Compared to AD patients, DLB patients showed lower CBF in the medial frontal, laterotemporal, biparietal, medial parietal (including precuneus) and occipital cortex (Figure 2). Furthermore, DLB patients showed lower CBF in the biparietal cortex, precuneus, and laterotemporal cortex compared to bvFTD patients. Voxel-based analyses showed no differences in uncorrected CBF between AD patients and bvFTD patients, nor did AD and bvFTD patients show lower uncorrected CBF compared to DLB patients. Similar results were found when comparing the PVC cortical CBF maps (Figure 3).

DISCUSSION

Patients with AD, DLB and bvFTD showed different patterns of regional CBF changes, measured by PCASL. In AD, CBF was decreased in all cerebral lobes, most prominently so in the posterior regions. Lowest overall CBF values were seen in DLB patients, but temporal CBF was preserved. BvFTD patients showed, except for the temporal lobes, overall moderate CBF changes that were most prominent in the frontal lobes. Voxel-wise CBF comparisons provided spatial maps visualizing the significant differences in CBF between the diagnostic groups.

To date, several studies have used a variety of different ASL sequences to examine absolute and relative perfusion in neurodegenerative diseases. Most of these studies focused on AD, and demonstrated that regions of decreased CBF are mainly located in the posterior cingulate cortex, precuneus and lateral parietal areas.[24-28] However, some of these studies also confirm the presence of a more diffuse pattern of functional changes in AD, including metabolic and perfusion changes in the frontal and temporal regions.[11, 24-26]

In this study, DLB patients showed the most severe and widespread CBF changes. Occipital hypoperfusion or hypometabolism is recognized as a supporting feature for the diagnosis of DLB in the current criteria.[29] A previous study that used a non-whole-brain ASL sequence to study perfusion in DLB patients confirmed this finding of parieto-occipital hypoperfusion in DLB patients compared to controls.[30] However, the single other study applying ASL to study CBF in DLB demonstrated that DLB patients showed decreases in CBF not only in the occipital lobes, but also in the frontal and parietal (including precuneus) lobes.[31] Furthermore, DLB patients showed a 10-12% reduction in CBF compared to AD patients. These findings are in line with our results, with DLB patients displaying diffuse CBF decreases (with relative preservation of the temporal parts of the brain) and lower CBF values than controls and patients

with AD and bvFTD. FDG-PET and SPECT literature also supports this finding of a widespread pattern of severe CBF changes in DLB,[32] even when compared to AD.[9, 33] Loss of acetylcholine-producing neurons in the basal forebrain is a common finding in DLB.[34] Since cholinergic neurons project not only to the cerebral cortex but to the cerebral blood vessels as well,[35] it has been suggested that regional hypoperfusion in DLB reflects reduced neuronal activity from both loss of cholinergic projections from subcortical neurons, and dynamic vascular effects. This double effect might contribute to the greater hypoperfusion in DLB patients compared to AD patients.[31]

Region-of-interest-based CBF comparisons showed different perfusion patterns in AD and FTD patients. Voxel-wise analyses displayed visually different distribution patterns of CBF changes in AD and bvFTD patients, but a direct voxel-wise comparison between AD and bvFTD did not reach significance, most probably due to lack of power. Two previous ASL studies comparing AD and FTD patients showed hypoperfusion in the precuneus and posterior cingulate cortex in AD patients.[36, 37] However, one of these studies only found these results when applying a relatively low threshold without a correction for multiple comparisons,[36] and in the other study FTD patients showed parietal hyperperfusion compared to controls, which increased the likelihood of detecting parietal hypoperfusion in AD compared to FTD.[37] The preservation of perfusion in the temporal lobes of FTD patients in this study is probably the result of our focus on behavioral variant FTD and exclusion of patients with severe to end-stage cortical atrophy in the right temporal lobe.

Currently, FDG-PET is the standard clinical imaging tool to assess functional changes in terms of hypometabolism in AD, FTD and DLB, and as such forms part of the diagnostic algorithm of memory clinic patients. The addition of FDG-PET to clinical information alone increases both diagnostic accuracy and physician confidence in AD and FTD diagnoses,[1] and the high specificity of FDG-PET in AD, FTD and DLB implies that negative or normal scan findings render a dementia diagnosis unlikely.[1] Since glucose metabolism and CBF are described to be closely related,[38, 39] ASL might become an important alternative for the visualization of cerebral (and neuronal) function. Although our results indicate that the pattern of PCASL measured regional CBF changes differ between AD, bvFTD and DLB on a group level, future studies are needed to clarify whether PCASL measured CBF is a distinctive marker on the individual level, and comparable to other modalities for predicting the correct diagnosis. Studies directly comparing these modalities in these disorders are needed to substantiate this claim.

This is the first study in which perfusion patterns of the three most common neurodegenerative diseases underlying dementia and age-matched controls are directly compared, by using a quantitative ASL MRI technique with whole-brain coverage. Both

CBF without correction for partial volume effects (representative for clinical practice) and PVC cortical CBF (actual gray matter CBF) were studied, in a region-of-interest and a voxel-wise fashion. The inclusion of subjects with subjective complaints instead of healthy controls might be considered a limitation. However, using subjects with subjective complaints as a control group provides the best reflection of a normal clinical situation. Furthermore, no controls with abnormal CSF Abeta were included. Additional potential limitations related to image technique include the fact that ASL scan quality could not be assured completely. Although the perfusion images were visually of good quality, the labeling efficiency was not assessed formally. Furthermore, we did not scan with several delay times to account for differences in travel times between groups. However, to alleviate the effect of delayed blood arrival in the brain of our study group (e.g. age, cerebrovascular co-morbidity, delayed transit time due to underlying pathology), we used a delay time of 2.0s instead of the commonly used 1.5s.[40]

We conclude that patients with AD, bvFTD and DLB exhibit distinct patterns of quantitative regional CBF changes. Being a non-invasive and easily accessible alternative for FDG-PET imaging, ASL may provide additional value in the workup of dementia and the differentiation between the most common types of neurodegenerative disorders that underlie dementia.

ACKNOWLEDGEMENTS

The authors thank Ajit Shankaranarayanan of GE Healthcare for providing the 3D pseudo-continuous ASL sequence that was used to obtain data for this paper. The study was supported by the Alzheimercenter of the VU University Medical Center Amsterdam, The Netherlands.

REFERENCES

1. Bohnen NI, Djang DS, Herholz K, Anzai Y, Minoshima S. Effectiveness and safety of 18F-FDG PET in the evaluation of dementia: a review of the recent literature. J Nucl Med 2012;53:59-71.
2. McKhann G, Drachman D, Folstein M, Katzman R, Price D, Stadlan EM. Clinical diagnosis of Alzheimer's disease: report of the NINCDS-ADRDA Work Group under the auspices of Department of Health and Human Services Task Force on Alzheimer's Disease. Neurology 1984;34:939-944.
3. McKeith IG, Dickson DW, Lowe J, et al. Diagnosis and management of dementia with Lewy bodies: third report of the DLB Consortium. Neurology 2005;65:1863-1872.
4. Neary D, Snowden JS, Gustafson L, et al. Frontotemporal lobar degeneration: a consensus on clinical diagnostic criteria. Neurology 1998;51:1546-1554.
5. Sluimer JD, van der Flier WM, Karas GB, et al. Accelerating regional atrophy rates in the progression from normal aging to Alzheimer's disease. EurRadiol 2009;19:2826-2833.
6. Whitwell JL, Josephs KA, Rossor MN, et al. Magnetic resonance imaging signatures of tissue pathology in frontotemporal dementia. Arch Neurol 2005;62:1402-1408.
7. Beyer MK, Larsen JP, Aarsland D. Gray matter atrophy in Parkinson disease with dementia and dementia with Lewy bodies. Neurology 2007;69:747-754.
8. Jack CR, Jr., Knopman DS, Jagust WJ, et al. Hypothetical model of dynamic biomarkers of the Alzheimer's pathological cascade. Lancet Neurol 2010;9:119-128.
9. Colloby SJ, Fenwick JD, Williams ED, et al. A comparison of (99m)Tc-HMPAO SPET changes in dementia with Lewy bodies and Alzheimer's disease using statistical parametric mapping. Eur J Nucl Med Mol Imaging 2002;29:615-622.
10. Lobotesis K, Fenwick JD, Phipps A, et al. Occipital hypoperfusion on SPECT in dementia with Lewy bodies but not AD. Neurology 2001;56:643-649.
11. Mosconi L, Tsui WH, Herholz K, et al. Multicenter standardized 18F-FDG PET diagnosis of mild cognitive impairment, Alzheimer's disease, and other dementias. J Nucl Med 2008;49:390-398.
12. Dai W, Garcia D, de Bazelaire C, Alsop DC. Continuous flow-driven inversion for arterial spin labeling using pulsed radio frequency and gradient fields. Magnetic resonance in medicine : official journal of the Society of Magnetic Resonance in Medicine / Society of Magnetic Resonance in Medicine 2008;60:1488-1497.
13. Binnewijzend MA, Kuijer JP, Benedictus MR, et al. Cerebral blood flow measured with 3D pseudocontinuous arterial spin-labeling MR imaging in Alzheimer disease and mild cognitive impairment: a marker for disease severity. Radiology 2013;267:221-230.
14. McKhann GM, Knopman DS, Chertkow H, et al. The diagnosis of dementia due to Alzheimer's disease: recommendations from the National Institute on Aging-Alzheimer's Association workgroups on diagnostic guidelines for Alzheimer's disease. Alzheimers Dement 2011;7:263-269.
15. Rascovsky K, Hodges JR, Knopman D, et al. Sensitivity of revised diagnostic criteria for the behavioural variant of frontotemporal dementia. Brain 2011;134:2456-2477.

16. Fazekas F, Chawluk JB, Alavi A, Hurtig HI, Zimmerman RA. MR signal abnormalities at 1.5 T in Alzheimer's dementia and normal aging. AJR AmJRoentgenol 1987;149:351-356.
17. Buxton RB, Frank LR, Wong EC, Siewert B, Warach S, Edelman RR. A general kinetic model for quantitative perfusion imaging with arterial spin labeling. Magnetic Resonance in Medicine 1998;40:383-396.
18. Smith SM. Fast robust automated brain extraction. HumBrain Mapp 2002;17:143-155.
19. Jenkinson M, Smith S. A global optimisation method for robust affine registration of brain images. MedImage Anal 2001;5:143-156.
20. Zhang Y, Brady M, Smith S. Segmentation of brain MR images through a hidden Markov random field model and the expectation-maximization algorithm. IEEE TransMedImaging 2001;20:45-57.
21. Asllani I, Borogovac A, Brown TR. Regression Algorithm Correcting for Partial Volume Effects in Arterial Spin Labeling MRI. Magnetic Resonance in Medicine 2008;60:1362-1371.
22. Nichols TE, Holmes AP. Nonparametric permutation tests for functional neuroimaging: a primer with examples. HumBrain Mapp 2002;15:1-25.
23. Smith SM, Nichols TE. Threshold-free cluster enhancement: addressing problems of smoothing, threshold dependence and localisation in cluster inference. Neuroimage 2009;44:83-98.
24. Alsop DC, Detre JA, Grossman M. Assessment of cerebral blood flow in Alzheimer's disease by spin-labeled magnetic resonance imaging. AnnNeurol 2000;47:93-100.
25. Dai W, Lopez OL, Carmichael OT, Becker JT, Kuller LH, Gach HM. Mild cognitive impairment and alzheimer disease: patterns of altered cerebral blood flow at MR imaging. Radiology 2009;250:856-866.
26. Johnson NA, Jahng GH, Weiner MW, et al. Pattern of cerebral hypoperfusion in Alzheimer disease and mild cognitive impairment measured with arterial spin-labeling MR imaging: initial experience. Radiology 2005;234:851-859.
27. Kim SM, Kim MJ, Rhee HY, et al. Regional cerebral perfusion in patients with Alzheimer's disease and mild cognitive impairment: effect of APOE Epsilon4 allele. Neuroradiology 2013;55:25-34.
28. Mak HK, Chan Q, Zhang Z, et al. Quantitative assessment of cerebral hemodynamic parameters by QUASAR arterial spin labeling in Alzheimer's disease and cognitively normal Elderly adults at 3-tesla. J Alzheimers Dis 2012;31:33-44.
29. McKeith IG. Consensus guidelines for the clinical and pathologic diagnosis of dementia with Lewy bodies (DLB): report of the Consortium on DLB International Workshop. J Alzheimers Dis 2006;9:417-423.
30. Taylor JP, Firbank MJ, He J, et al. Visual cortex in dementia with Lewy bodies: magnetic resonance imaging study. Br J Psychiatry 2012;200:491-498.
31. Fong TG, Inouye SK, Dai W, Press DZ, Alsop DC. Association cortex hypoperfusion in mild dementia with Lewy bodies: a potential indicator of cholinergic dysfunction? Brain Imaging Behav 2011;5:25-35.
32. Ishii K, Soma T, Kono AK, et al. Comparison of regional brain volume and glucose metabolism between patients with mild dementia with lewy bodies and those with mild Alzheimer's disease. J Nucl Med 2007;48:704-711.

33. Shimizu S, Hanyu H, Kanetaka H, Iwamoto T, Koizumi K, Abe K. Differentiation of dementia with Lewy bodies from Alzheimer's disease using brain SPECT. Dement Geriatr Cogn Disord 2005;20:25-30.
34. Albin RL, Minoshima S, D'Amato CJ, Frey KA, Kuhl DA, Sima AA. Fluoro-deoxyglucose positron emission tomography in diffuse Lewy body disease. Neurology 1996;47:462-466.
35. Sato A, Sato Y, Uchida S. Regulation of cerebral cortical blood flow by the basal forebrain cholinergic fibers and aging. Auton Neurosci 2002;96:13-19.
36. Du AT, Jahng GH, Hayasaka S, et al. Hypoperfusion in frontotemporal dementia and Alzheimer disease by arterial spin labeling MRI. Neurology 2006;67:1215-1220.
37. Hu WT, Wang Z, Lee VM, Trojanowski JQ, Detre JA, Grossman M. Distinct cerebral perfusion patterns in FTLD and AD. Neurology 2010;75:881-888.
38. Chen Y, Wolk DA, Reddin JS, et al. Voxel-level comparison of arterial spin-labeled perfusion MRI and FDG-PET in Alzheimer disease. Neurology 2011;77:1977-1985.
39. Jueptner M, Weiller C. Review: does measurement of regional cerebral blood flow reflect synaptic activity? Implications for PET and fMRI. Neuroimage 1995;2:148-156.
40. Campbell AM, Beaulieu C. Pulsed arterial spin labeling parameter optimization for an elderly population. J Magn Reson Imaging 2006;23:398-403.